Time Resolved Imaging of Spin Transfer Switching: Beyond the Macro-Spin Concept

Y. Acremann,[1] J.P. Strachan,[2] V. Chembrolu,[2] S.D. Andrews,[3] T. Tyliszczak,[4]

J.A. Katine,[5] M.J. Carey,[5] B.M. Clemens,[3] H.C. Siegmann,[1] and J. Stöhr[1]

[1]*Stanford Synchrotron Radiation Laboratory, Stanford, California 94309, USA*

[2]*Department of Applied Physics, Stanford University, Stanford, California 94305, USA*

[3]*Department of Materials Science and Engineering,*

Stanford University, Stanford, California 94305, USA

[4]*Advanced Light Source, Berkeley, California 94720, USA*

[5]*Hitachi Global Storage Technologies,*

San Jose Research Center, San Jose, California 95120, USA

(Dated: May 8, 2006)

Abstract

Time resolved images of the magnetization switching process in a spin transfer structure, obtained by ultrafast x-ray microscopy, reveal the limitations of the macrospin model. Instead of a coherent magnetization reversal, we observe switching by lateral motion of a magnetic vortex across a nanoscale element. Our measurements reveal the fundamental roles played independently by the torques due to charge and spin currents in breaking the magnetic symmetry on picosecond timescales.
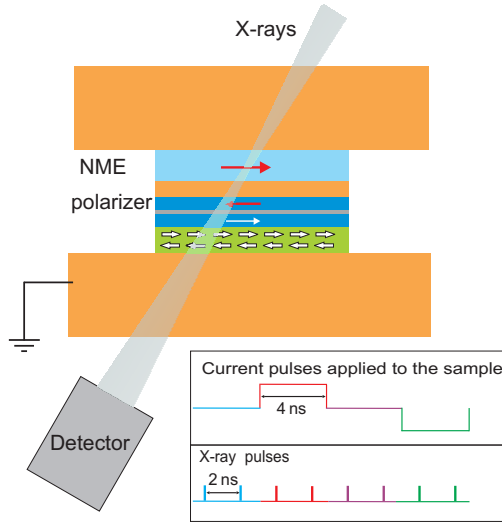
FIG. 1: Schematic of the experiment. The pillar structure with the NME is shown including the Cu contacts on top and bottom. The current is spin polarized by the polarizer layer. The incident monochromatic x-ray beam is focused to a spot size of $\approx 30\text{nm} \times 30\text{nm}$ and the transmitted intensity is measured as a function of the beam position. The pump-probe timing scheme is shown at the bottom.

Reversal of the magnetization $\vec{M}$ in nanoscale magnetic elements (NME) is one of the basic operations in advanced applications of magnetism today. The presently used method of switching NMEs by external magnetic field pulses is envisioned to be replaced by direct injection of spin polarized currents [1–7]. Such spin switching has indeed been observed in giant magneto-resistance (GMR) studies following a stepwise change in the injected spin current [8–10], and spontaneous radiofrequency emission has also been detected [11–15]. So far, however, the evolution of the nanoscale magnetization distribution during the switching process has remained hidden. Here we report the first direct observation of the detailed magnetic switching process in space and time using advanced pump-probe x-ray microscopy. Motion pictures with 200 ps time resolution reveal a sub-nanosecond switching process where a magnetic vortex created by the Oersted field of the charge current is shifted across the NME by the spin current. As the vortex core leaves the NME, a C-state is formed which may later decay deterministically into a uniform magnetic state.

Our sample consisted of a 4 nm thick NME with an elliptical cross section of $100\,\text{nm} \times 150\,\text{nm}$, sandwiched between other layers and buried under current leads in a typical CPP-spin valve pillar [16], as illustrated in Fig. 1. Current pulses of $2 \times 10^8\,\text{A/cm}^2$[27] provided
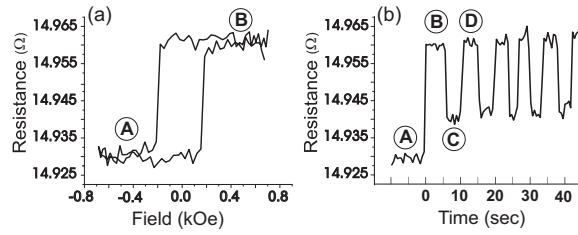
FIG. 2: GMR measurements of field and current pulse induced switching. As shown in (a) the sample shows a square GMR-hysteresis loop in an external field, indicating a uniform saturation magnetization. With current pulses of 4 ns length, as applied in the pump-probe x-ray microscopy measurements, the sample exhibits a full change of GMR only on the first current pulse (A to B). The measurement time between pulses is 5 seconds. Subsequent set (B to C) and reset (C to D) pulses show a lower GMR effect, indicating the creation of a non-saturated intermediate metastable structure C.

by a pulse generator flow perpendicular to the pillar from the top to the bottom or vice versa, depending on the sign of the voltage applied to the Cu electrodes. The NME of interest consists of $Co_{0.86}Fe_{0.14}$. The multilayer structure below the NME is designed to spin-polarize the current while minimizing magnetic coupling to the NME. The two ferromagnetic (FM) layers whose magnetization stays fixed consist of 2 nm $Co_{0.86}Fe_{0.14}$, separated by an interlayer of 0.7 nm Ru which couples their magnetizations antiparallel. The top FM layer labeled polarizer is responsible for the direction and magnitude of the spin polarization of the current. Its magnetization direction is pinned by the coupling to the lower FM layer which in turn is exchange biased by a PtMn antiferromagnet. A spacer layer of 3.5 nm Cu interrupts the exchange coupling between the NME and the polarizer. The whole multilayer structure rests on a 300 nm thick SiN membrane (not shown in Fig.1) which is largely transparent to x-rays. The sample fabrication involved techniques developed at Hitachi for use in magnetic readout sensors [16].

In an external magnetic field, square GMR magnetization loops are obtained as shown in Fig. 2 (a), indicating that uniform magnetic structures have been reached at the maximum field values. The loops are shifted on the field axis showing that there is residual coupling by the stray field from the polarizer of $H_{sf} \approx -50$ Oe at the location of the NME, favoring antiparallel alignment of the NME with respect to the polarizer. Injecting a positive spin current pulse (electrons flow from the polarizer to the NME) of 4 ns duration followed by

3

a negative spin current reset pulse, as used for magnetic switching, is expected to yield reproducible, constant jumps of GMR of the same magnitude as obtained by switching $\vec{M}$ in an external field. As illustrated in Fig. 2 (b), the first current induced GMR jump from point A to B has indeed the same magnitude as the field induced jump, consistent with uniform $\vec{M}$ reversal. However, subsequent current injections (sequence B to C to D etc.) exhibit reduced GMR jumps, indicating that a different $\vec{M}$ state (e.g. point C) has been created. This intermediate state is metastable. The original large GMR jump (A to B) is recovered only after the structure has been realigned by an external magnetic field. The nature of the intermediate state, as well as the mechanism leading to it, remains hidden in GMR. This demonstrates that spatially resolved information of the magnetization is required to fully understand reversal by spin injection.

Images of $\vec{M}(x, y, t)$ where x and y are coordinates in the plane of the NME and t is the time, are obtained by scanning transmission x-ray microscopy (STXM) [17] as shown in Fig. 1. The circularly polarized x-ray beam from an undulator on beam line 11.0.2 at the Advanced Light Source (ALS) is incident 30° from the surface normal. It is focused to $\approx$ 30 nm by a zone plate. The transmission of the x-rays through the whole pillar is monitored by a fast avalanche detector as a function of the position x, y while the pillar is scanned in steps of 10 nm across the x-ray focus. Tuning the photon energy to the characteristic Co L_3 resonance provides magnetic contrast through the x-ray magnetic circular dichroism (XMCD) effect [18]. The M_x and M_y components of $\vec{M}$ are obtained by rotating the pillar by 90° in the x-y plane. 4 ns positive (set) and 4 ns negative (reset) current pulses separated by 4 ns are applied to the sample by two pulse generators. The rise time of the current pulses is 200 ps. The current pulse sequence is synchronized with the x-ray pulses which appear every 2 ns. A special photon counting system allows us to measure the differences of the magnetizations $\vec{M}_i - \vec{M}_j$ for each pair of eight consecutive x-ray pulses, suppressing slower drifts and sample vibrations. The delay of the 75 ps wide x-ray pulses to the current pulse sequence can be changed in order to measure the time evolution of the magnetization.

We know from the GMR data that the fully saturated uniform state $\vec{M}^0$ (points B and D) is reached either by application of a field or after the reset pulse (e.g. C to D). With this reference state as input, the other $\vec{M}$ states can be reconstructed from the appropriate difference measurements.

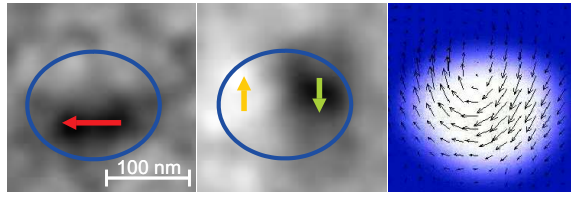As an example, we show in Fig. 3 the spatial variation of $\vec{M} = (M_x, M_y)$, recorded

4

FIG. 3: Stationary magnetic images recorded 2 ns after the rising edge of the set-pulse. The magnetic images containing M_x (horizontal, a) and M_y (vertical, b) combine into the vector field (c) which represents the direction of the magnetization. The length of the arrows indicates the observed magnitude of the magnetic contrast.

2 ns after the rising edge of the set-current pulse. The length of the arrows represents the XMCD contrast from the combined orthogonal images in the x (horizontal) and y (vertical) directions. Note that the length of the arrows is influenced by the spatial resolution and does not represent $|\vec{M}|$. To our knowledge, this is the first time that the magnetic structure in a spin injection pillar has been observed. Obviously, the magnetization is not uniform, but is bent into a C-state.

The time evolution of the magnetization near the onset of the current pulses reveals a novel magnetization switching mechanism and is shown in Fig. 4 (a - i). The changes of the magnetization happen within a few hundred picoseconds after the 200 ps onset of the pulse sequence. The initial magnetization is uniform (4a). The positive current pulse causes the magnetization to bend upwards (4b), forming a vortex. As this vortex moves through the NME, it leaves behind a trail of reversed magnetization. As the vortex center leaves the magnetic structure, a C-state (4c) is formed. The end of the positive set pulse has no noticeable effect, showing that the C-state (4d) is a metastable configuration. The negative pulse first leads to an almost uniform magnetization, caused by injection of a new vortex with opposite curl into the NME (4e). The new vortex moves through the NME and reverses its magnetization (4f). The new C-state with M_x antiparallel to the polarizer is not stable at zero current but relaxes relatively slowly into the original uniform configuration (4g - i).

Recent numerical simulations [19, 20] as well as dynamical experiments using GMR [21] have suggested that the Oersted field caused by the charge current produces a transient curled magnetization distribution in the NME. Our experiment demonstrates that C-states of various shapes are indeed generated. The C-state, shown in Fig. 4d, which is bistable with the uniform state, can solely be reached by injection of a current, but not by application
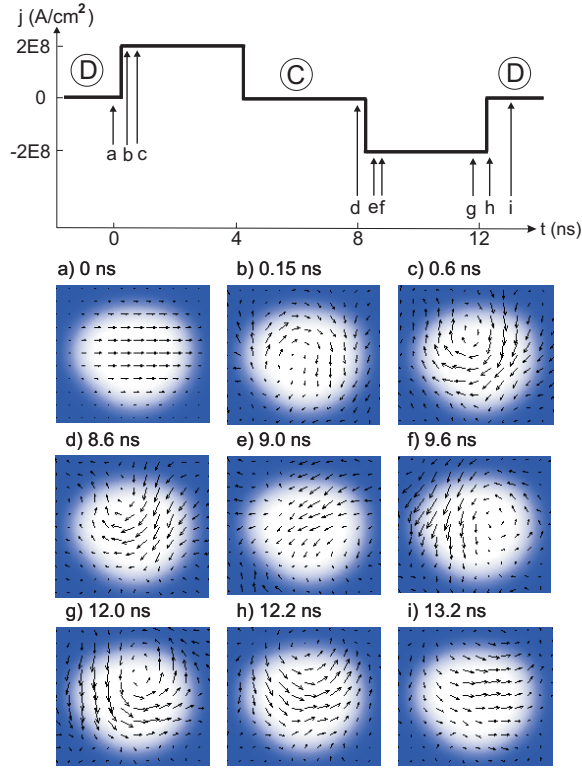
5

FIG. 4: Evolution of the magnetization during the pulse sequence. The uniform anti-parallel configuration (a) is switched into a C-state with parallel M_x component (c). The switching process involves motion of a magnetic vortex through the NME, visible in (b). The C-state is metastable after the falling edge of the pulse (d) and is reversed by the reset-pulse into another C-state (f). The switching of one C-state into another is caused by lateral vortex motion as well, leaving a uniformly magnetized area in the center of the NME (e). The C-state with its horizontal x-component antiparallel to the polarizer is unstable and relaxes into the uniform state (g - i). This relaxation is deterministic but comparatively slow. The labels (D) and (C) indicate the states of figure 2.

of an external field. The detailed modelling of these observations requires numerical studies which are beyond the scope of this paper. Below we instead give physical arguments in support of the observed results.

The NME has a thickness of t and an elliptical shape with major radius $R_1 = 75\,\mathrm{nm}$ and minor radius $R_2 = 50\,\mathrm{nm}$. Between the pulses, the uniform magnetization is almost degenerate with the vortex or C-state [22, 23]. At our current density of $2 \times 10^8 \mathrm{A/cm^2}$, the Oersted field has a maximum value of $\approx 950\,\mathrm{Oe}$ and favors the formation of the ob-

6

served curled magnetic states over the uniform configuration. The size and thickness of the NME determines the ratio of the energies of the uniform state and the C-state [22], as well as the ratio of the torques due to H_{Oe} and the injected spins. Therefore, the switching process observed by us may differ from that in pillars with different internal structures and dimensions.

The observed switching process by displacement of a magnetic vortex follows a path of low energy. Our sample has a shape anisotropy of $H_{\text{ani}} \approx 200\,\text{Oe}$ (Fig 2). The energy barrier for switching by uniform rotation is $E_R = \frac{1}{2}H_{\text{ani}}|M|R_1 R_2 \pi t$. In contrast, the energy cost for switching by the motion of a magnetic vortex can be estimated by assuming that the C-state is degenerate in energy with the uniform state. The energy barrier for switching by vortex motion can be estimated as the energy to create a vortex core of radius $r_c \approx 5\,\text{nm}$ [24] within the sample. The vortex core is created to accommodate the exchange energy in the center of the vortex and costs the stray field energy of a perpendicularly magnetized disk of radius r_c, namely $E_V \approx \frac{M_s^2}{2\mu_0}r_c^2 \pi t$. With $|M| \approx 2\,\text{T}$, we obtain the ratio $P = \frac{E_V}{E_R} = 0.17$. Thus the energy barrier for switching by vortex motion compared to the barrier of uniform rotation is reduced by a factor of five.

In the final uniform state reached after the reset pulse, $\vec{M}$ is antiparallel to the magnetization $\vec{M}_P$ in the polarizer. The uniform state is thus stabilized by the stray field of the polarizer. In contrast, the C-state of Fig. 4c forms when $\vec{M}$ is parallel to $\vec{M}_P$ and in this case the stray field opposes and destabilizes a potential uniform state. Based on our experience with other samples, the possible relaxation of the C-state into the uniform state depends on fine details of the magnetic couplings and other properties of the nano-pillar. The particular sample presented in this paper has been chosen because one of the states is uniform, allowing the reconstruction of the magnetization $\vec{M}_i$ from the measured difference images $\vec{M}_i - \vec{M}_j$.

Our experiment shows that vortex dynamics, previously observed in micrometer-sized magnetic structures [25, 26], can also dominate the switching mechanism in the nanometer-sized elements in spin transfer nanopillars. Two kinds of symmetry breaking effects work hand-in-hand. First, the curled Oersted field breaks the mirror symmetry along the spin direction and creates a non-zero torque on the magnetization of the NME immediately after the rising edge of the current pulse, so that no thermal fluctuations are needed to initiate switching. In response to the Oersted field a vortex state is formed. Second, the spin

polarized current, aligned into a unique direction by the polarizer, simply shifts the vortex so that its center lies outside the sample. This motion is expected to involve precessional motion of the magnetization, as well, but this is fast and cannot be resolved within our time resolution. The combined actions of the Oersted field and spin injection explain the short switching time of $\approx 500\,\mathrm{ps}$ observed here and the even faster times of $100\,\mathrm{ps}$ observed previously [21]. The switching speed of $500\,\mathrm{ps}$ leads to a vortex speed of about $150\,\mathrm{m/s}$, consistent with other observations [25]. Finally, we note that the non-thermally initiated switching process is deterministic and therefore desirable in switching applications.

[1] J. C. Slonczewski, J. Magn. Magn. Mater **159**, L1 (1996).

[2] L. Berger, Phys. Rev. B **54**, 9353 (1996).

[3] M. Tsoi, A. G. M. Jansen, J. Bass, W. C. Chiang, M. Seck, V. Tsoi, and P. Wyder, Phys. Rev. Lett. **80**, 4281 (1998).

[4] J. Z. Sun, J. Magn. Magn. Mater **202**, 157 (1999).

[5] E. B. Myers, D. Ralph, J. A. Katine, R. N. Louie, and R. A. Buhrman, Science **285**, 867 (1999).

[6] J. A. Katine, F. J. Albert, R. A. Buhrman, E. B. Myers, and D. C. Ralph, Phys. Rev. Lett. **84**, 3149 (2000).

[7] J. Grollier, V. Cros, A. Hamzic, J. M. George, H. Jaffres, A. Fert, G. Faini, J. B. Youssef, and H. Legall, Appl. Phys. Lett. **78**, 3663 (2001).

[8] R. H. Koch, J. A. Katine, and J. Z. Sun, Phys. Rev. Lett. **92**, 88302 (2004).

[9] I. N. Krivorotov, N. C. Emley, J. C. Sankey, S. I. Kiselev, D. C. Ralph, and R. A. Buhrman, Science **307**, 228 (2005).

[10] T. Devolder, A. Tulapurkar, K. Yagami, P. Crozat, C. Chappert, A. Fukushima, and Y. Suzuki,

J. Magn. Magn. Mater **286**, 77 (2005).

[11] M. Tsoi, A. G. M. Jansen, J. Bass, W. C. Chiang, V. Tsoi, and P. Wyder, Nature **406**, 46 (2005).

[12] S. L. Kiselev, J. C. Sankey, I. N. Krivorotov, N. C. Emley, R. J. Schoelkopf, and R. A. Buhrman, Nature **425**, 380 (2003).

[13] W. H. Rippard, M. R. Pufall, S. Kaka, S. E. Russek, and T. J. Silva, Phys. Rev. Lett. **92**, 027201 (2004).

[14] S. I. Kiselev, J. C. Sankey, I. N. Krivorotov, N. C. Emley, M. Rinkoski, C. Perez, R. A. Buhrman, and D. C. Ralph, Phys. Rev. Lett. **93**, 036601 (2004).

[15] M. Covington, M. AlHajDarwish, Y. Ding, N. J. Gokemeijer, and M. A. Seigler, Phys. Rev. B **69**, 184406 (2004).

[16] D. Lacour, J. A. Katine, N. Smith, M. J. Carey, and J. R. Childress, Appl. Phys. Lett. **85**, 4681 (2004).

[17] A. L. D. Kilcoyne, T. Tyliszczak, W. F. Steele, S. Fakra, P. Hitchcock, K. Franck, E. Anderson, and B. Harteneck, J. Synchr. Rad. **10**, 125 (2003).

[18] J. Stöhr, Y. Wu, B. D. Hermsmeier, M. G. Samant, G. R. Harp, S. Koranda, D. Dunham, and B. Tonner, Science **259**, 658 (1993).

[19] B. Hillebrands and A. Thiaville, eds., *Spin Transfer Torque and Dynamics, in Spin Dynamics in Confined Structures III* (Springer, 2005).

[20] L. Torres, L. Lopez-Diaz, E. Martinez, M. Carpentieri, and G. J. Finocchi, J. Magn. Magn. Mater **286**, 381 (2005).

[21] T. Devolder, A. Tulapurkar, Y. Suzuki, C. Chappert, P. Crozat, and K. Yamagi, J. Appl. Phys. **98**, 053904 (2005).

[22] S. Urazhdin, C. L. Chien, K. Y. Guslienko, and L. Novozhilova, Phys. Rev. B **73**, 054416 (2006).

[23] H. F. Ding, A. K. Schmid, D. Li, K. Y. Guslienko, and S. D. Bader, Phys. Rev. Lett. **94**, 157202 (2005).

[24] A. Wachowiak, J. Wiebe, M. Bode, O. Pietzsch, M. Morgenstern, and R. Wiesendanger, Science **298**, 577 (2002).

[25] S. B. Choe, Y. Acremann, A. Scholl, A. Bauer, A. Doran, J. Stöhr, and H. A. Padmore, Science **304**, 420 (2004).

[26] B. V. Waeyenberge et al., to be published (2006).

[27] This current density corresponds to twice the current density required to switch the magnetization by a DC current.